International Journal of Materials Chemistry and Physics
Vol. 1, No. 3, 2015, pp. 366-369
http://www.aiscience.org/journal/ijmcp

Sintering Effect on Structural and Electrical Properties of $Zn_xFe_{1-x}Fe_2O_4$ Ferrite Nano-particles

Amarjeet[1, 2], Vinod Kumar[2, *]

[1]Department of Physics, JVMGRR College, Ch. Dadri, India
[2]Department of Physics, DCR University of Science and Technology, Murthal, India

Abstract

$Zn_xFe_{1-x}Fe_2O_4$ nano spinel ferrites with composition x = 0.2, 0.6, 0.8 and 1 were prepared by chemical co-precipitation method keeping pH equal to 8. Synthesized samples were sintered at 673 K and 873 K for two hours each separately in a muffle furnace at slow rate of heating and cooling. Sintered samples were characterized by Fourier transform infra-red (FTIR) at room temperature in the range 4000 cm^{-1} to 400 cm^{-1}. The recorded infra-red (IR) absorption spectra provided the structural information of sintered samples. Fourier transform infra-red absorption spectra confirmed the single phase formation and cubic spinel structure existence in the all sintered samples. The dc conductivity decreases with increase in sintering temperature. Direct current (DC) conductivity first increases with increase in zinc content and then decreases with further increase in zinc content. The study of temperature dependence behaviour showed semiconducting nature of the sintered samples.

Keywords

Nano, Spinel Ferrites, Co-precipitation, Sintering, FTIR

Received: September 3, 2015 / Accepted: September 24, 2015 / Published online: December 6, 2015

1. Introduction

The general formula of spinel ferrites is represented by AB_2O_4 and it possesses 64 tetrahedral sites (A-site) and 32 octahedral (B-site). Spinel ferrites possess unique electrical properties for wide range of technological applications. The electrical properties of nano ferrites are improved in comparison to their bulk counterparts. Nano ferrites have applications in the area of magnetic recording media, ferro-fluids, magnetic recording media, ferro-fluids, magnetic resonance imaging, multilayer chip indicator, etc. Nano ferrites act as potential candidates for microwave devices due to high resistivity and low eddy current losses at high frequency [1]. The dielectric and magnetic properties of ferrites are dependent on microstructure, chemical composition and synthesis technique [2]. There are several synthesis techniques for the synthesis of nano-crystalline particles such as solid-state reaction method, hydrothermal method, reverse-micelle method, sol-gel, auto-combustion method and chemical co-precipitation method [3, 4]. It is important to adopt a synthesis technique that provides nano sized particles with high chemical purity. The chemical co-precipitation method is low cost, provides the high yield and homogenous particle size distribution of the nano-ferrite particles [4]. Therefore, we have $Zn_xFe_{1-x}Fe_2O_4$, (with x = 0.2, 0.6, 0.8 and 1.0) were synthesized by chemical co-precipitation method. The developed particles were then annealed at 673 K and 873 K separately in a muffle furnace for two hour at slow heating rate 5 K per minute and cooled with same rate after sintering. The developed annealed samples were further studied for structural and electrical properties.

2. Experimental

Zn-Fe ferrite nano-particles with different Zn^{2+} to Fe^{2+} ion ratio were synthesized using chemical co-precipitation

* Corresponding author
E-mail address: vinod.phy@dcrustm.org (V. Kumar)

method with formula $Zn_xFe_{1-x}Fe_2O_4$, where x = 0.2, 0.6, 0.8 and 1.0. $ZnCl_2$, Fe $(NO_3)_3.9H_2O$ and $FeCl_2$ were taken as starting materials with high purity (99%). After calculations of each initial material, separate solutions were prepared for Zn(II) and Fe(III) and heated with magnetic stirring for two hour and all solutions were then mixed and again heated with magnetic stirring for proper mixing for sufficient time. After proper mixing, small quantity of surfactant was added in prepared solution and then stirred again for sufficient time. For precipitation of such prepared solution, ammonia was added in solution drop by drop with continuous stirring. Precipitated samples were heated at 80°C to get dry. The nano-size of the spinel ferrite particles by chemical co-precipitation method was already confirmed in previous research works [4]. Prepared particles were sintered at 673 K and 873 K separately for two hour in a muffle furnace with temperature rising and cooling at rate 5 K per minute and then crushed to get powder form for characterization purposes. Annealed samples were studied for IR properties in the range 4000 to 400 cm^{-1} through KBR pallet technique using an FTIR (Perkin Elmer Frontier).

DC measurements were carried out in a wide range of temperature using a Keithley 2401 source cum electrometer and a programmable pot furnace in wide range of temperature in the order of decreasing temperature to remove the effect of humidity from the samples. For this measurement, all sintered samples were palletized using a palletizer of 13 mm diameter under the same pressure for the same time.

3. Results and Discussion

3.1. IR Results Analysis

Figure 1 and figure 2 shows FTIR absorption spectra of spinel ferrites $Zn_xFe_{1-x}Fe_2O_4$ annealed at 673 K and 873 K respectively with composition x = 0.2, 0.6, 0.8 and 1. The IR absorption spectra of each composition consists of two significant absorption bands which reveal the formation of single phase of spinel ferrites having two sub lattices, tetrahedral and octahedral sites [5]. The occurrence of first band at higher wave number, ν_1 of nearly 550 cm^{-1} is due to the intrinsic vibrations of the tetrahedral complexes (M-O bond vibrations) and the second band at lower wave number, ν_2 of nearly 466 cm^{-1} is due to the intrinsic vibrations of the octahedral complexes (M-O bond vibrations) [6]. The difference in frequencies of two characteristics bands of ferrites is due to the long bond length of oxygen-metal ions in the octahedral sites and shorter bond length in the tetrahedral sites [7]. The bands around 1600 cm^{-1}, 3400 cm^{-1} and 2900 cm^{-1} are due to O-H stretching vibrations bonds [8].

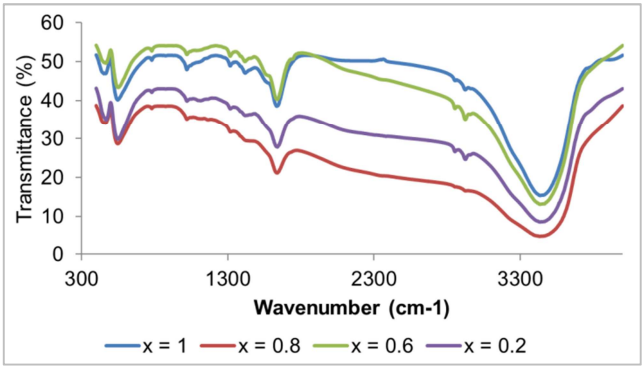

Fig. 1. FTIR spectra of samples $Zn_xFe_{1-x}Fe_2O_4$ annealed at 673 K.

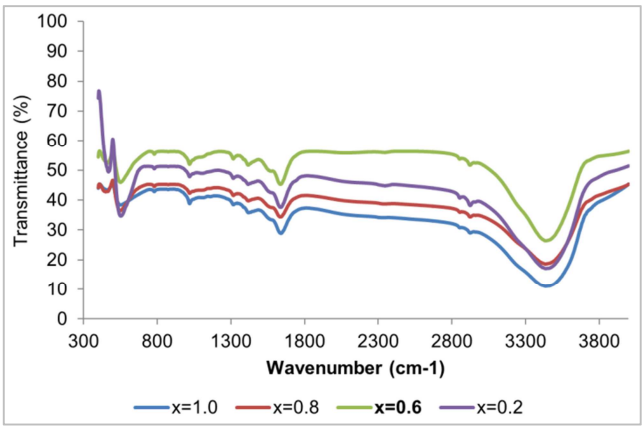

Fig. 2. FTIR spectra of samples $Zn_xFe_{1-x}Fe_2O_4$ annealed at 873 K.

Table 1 shows the variation in tetrahedral and octahedral vibration wave numbers with the content of zinc and sintering temperature. In table 1, ν_1 and ν_2 are tetrahedral and octahedral vibration wave numbers respectively for samples sintered at 673 K and ν'_1, ν'_2 are tetrahedral and octahedral vibration wave numbers respectively for samples sintered at 873 K. From the table 1, it has been observed that ν_1, ν_2, ν'_1 and ν'_2 shift slightly towards lower wave number with the increase in zinc concentration (x) due to the sintering on the samples [9]. The shift in the characteristics band wave numbers ν_1, ν_2, ν'_1 and $\nu'_2$is due to change in the M-O inter nuclear distances for the tetrahedral and octahedral sites respectively [10-11]. The shifting in wave numbers of tetrahedral and octahedral vibrations may be also due to removal of stress/strain during sintering the samples. During sintering, different parameters tend to get their standard values due to the removal of stresses and strains.

Table 1. Variation in tetrahedral and octahedral vibration wave numbers with the content of zinc and sintering temperature.

Zinc content (x)	Tetrahedral frequency, ν_1 (cm^{-1})	Octahedral frequency, ν_2 (cm^{-1})	Tetrahedral frequency, ν'_1 (cm^{-1})	Octahedral frequency, ν'_2 (cm^{-1})
0.2	550	467	553	469
0.6	549	466	550	466
0.8	548	465	549	465
1.0	548	465	548	465

3.2. DC Results Analysis

All the prepared samples sintered at 673 K and 873 K were palletized using a palletizer of 13 mm diameter under equal pressure of hydraulic press for equal interval of time. The samples were polished to obtained parallel surfaces, which were coated with silver paste for good electrical contacts. The samples were inserted between two electrodes of sample holder in a potable furnace. The variations of the electric current with applied dc voltage were recorded for all sintered samples in a wide range of temperature.

From the experimental results of the V-I characteristics, the resistance was determined at each temperature from the slope of line as per Ohm`s law. Then dc conductivity was measured as function of temperature for all compositions for both sintered temperatures 673 K and 873 K as shown in figure 3 and figure 4. The relationship between log σdc and 1000/T is given according to Wilson`s equation (1) as:

$$\sigma_{dc} = \sigma_0 \exp[-E/K_BT], \quad (1)$$

where σ_0 is constant, σ is electrical conductivity at temperature T, E is activation energy and K_B is Boltzman`s constant. Equation shows that as temperature increases, conductivity increases for all samples showing semiconducting nature of the samples.

DC conductivity first increases with increase in zinc content up to x = 0.6 and then decreases. The non-magnetic Zn^{2+} ion prefers the occupation of tetrahedral (A) sites [12, 13-18], while magnetic Fe ion partially occupies A- and B-sites [12, 13-21]. The electron hopping between Fe^{2+} and Fe^{3+} ions are responsible for electric conduction in ferrites [22, 23]. The increase in conductivity with increase in Zn content may be due to increase in crystalline size and hence decrease in the band gap. With the further increase in Zn content, Fe^{2+} ions are more decreased which decreases electron hopping between Fe^{2+} and Fe^{3+} ions and hence conductivity decreases as Zn^{2+} ion substitution increases replacing Fe^{2+} ions.

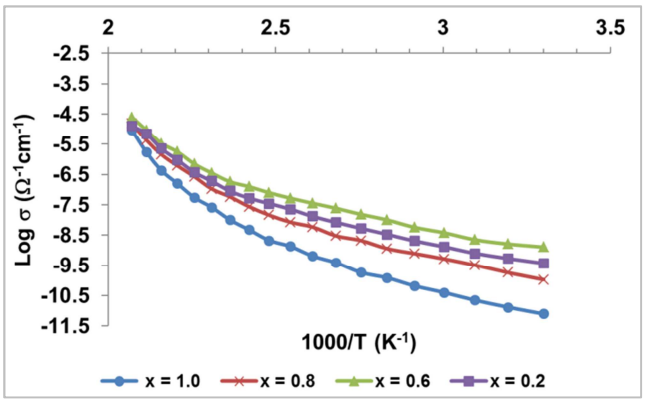

Fig. 3. Variation of dc conductivity with temperature of samples $Zn_xFe_{1-x}Fe_2O_4$ annealed at 673 K.

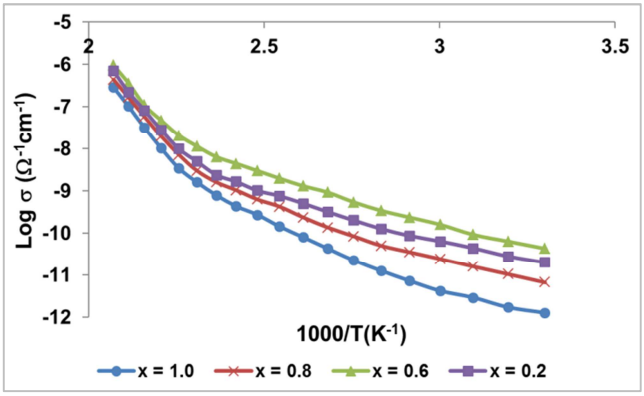

Fig. 4. Variation of DC conductivity with temperature of samples $Zn_xFe_{1-x}Fe_2O_4$ annealed at 873 K.

Analysis of figure 3 and figure 4 show that dc conductivity decreases with increase in sintering temperature. Dc conductivity is higher at lower sintering temperature 673 K then 873 K. This may be due to the formation of grains and fewer defects during sintering [24]. The decrease in conductivity with further increase in Zn content may also be due to formation of defects.

4. Conclusion

Polycrystalline ferrite particles $Zn_xFe_{1-x}Fe_2O_4$ with composition x = 0.2, 0.6, 0.8 and 1 prepared by chemical co-precipitation method and sintered at different temperatures were studied for structural and electrical properties. The FTIR absorption spectra of each composition consists of two significant absorption bands which reveal the formation of single phase of sintered spinel ferrites having two sub lattices, tetrahedral and octahedral sites. The temperature dependence behaviour of dc conductivity shows that sintered samples are semiconducting in nature. Dc conductivity decreases with the increase in sintering temperature which may be due to the formation of grains and fewer defects during sintering.

Acknowledgement

The authors are thankful to coordinator CIL, DCRUST, Murthal for providing basic facilities for FTIR and DC conductivity measurements.

References

[1] J. Kulikowski, J. Magn. Magn. Mater. 41, 56 (1984).

[2] A. Verma and R. Chatterjee, J. Magn. Magn. Mater. 306, 313 (2006).

[3] W. Y. Huang, P. Y. Du, W. J. Weng and G. R. Han, J. Mater. Sci. Eng. 23, 528 (2005).

[4] Vinod Kumar, Anu Rana, M. S. Yadav and R. P. Pant, J. Mag. Mag. Mater. 320, 1729 (2008).

[5] Erum Pervaiz and I. H. Gul, J. Mag. Magn. Mat. 324 (22), 3695 (2012).

[6] B. P Jacob, Smitha Thankachan, Sheena Xavier and E. M. Mohammed, Phys Scripta. 84, 045702 (2011).

[7] O. S. Josyulu and J. Sobhanadri, Phys Stat Sol., (a) 65(2), 479 (1981).

[8] H. I. Hsiang, Chih-Cheng Chen and W. Yue Tsai, Appl. Surface Sci. 245(1-4), 252 (2005).

[9] J. Balavijayalakxmi, N. Suryanarayanan and R. Jayaprakash, J. Mag. Magn. Mater. 362, 135 (2014).

[10] R. D. Shannon, Acta Cryst. A32, 751 (1976).

[11] F. J. W. Verwey and J. H. De Boer, Rec. Trav. Chem. Pays Bas. 55, 531 (1936).

[12] G. K. Joshi, S. A. Deshpande, A. Y. Khot, S. R. Sawant, Ind. J. Appl. Phys. A 61, 251 (1987).

[13] B. V. Bhise, M. B. Dongar, S. A. Patil, S. R. Sawant, J. Mater. Sci. Lett. 10 (1991).

[14] G. K. Joshi, A. Y. Khot, S. R. Sawant, Solid State Commun. 65 (1988).

[15] H. D. Patil, R. V. Upadhyay, N. R. Shamkumar, R. G. Kulkarni, Solid State Commun. 81, 1001 (1992).

[16] M. N. Khan, A. Ahmad, V. S. Darshane, J. Mater. Sci. 24, 163 (1989).

[17] M. Arshed, N. B. Buit, M. Siddique, A. Anwar-Ul Islam, T. Abbas, M. Ahmed, Solid State Commun. 84, 717 (1992).

[18] F. Grandjean, A. Gerard, Solid State Commun. 25, 679 (1978).

[19] T. E. Whall, N. Salerno, Y. G. Proykova, V. A. M. Babers, Philos. Mag. 53, L167 (1986).

[20] J. S. Bijal, S. Phanjouban, D. Kothari, C. Prakash, P. Kishan, Solid State Commun. 83, 679 (1992).

[21] R. B. Jotania, R. V. Upadhay, R. G. Kulkarni, IEEE Trans. Magn. 28, 1889 (1992).

[22] P. V. Reddy, T. S. Rao, S. M. D. Rao, J. Less-Common Met. 79, 191 (1981).

[23] Naveen Kumari, Vinod Kumar, S. K. Singh, Cer. Inter. 40, 12199 (2014).

[24] B. Gillot, Phys. Stat. Solidi (a) 76, 601 (1983).